

Studying the Ionospheric Responses Induced by a Geomagnetic Storm in September 2017 with Multiple Observations in America

Yang Liu^{1,*}, Zheng Li¹, Jinling Wang²

¹School of Instrumentation and Opto-electronic, Beihang University, Beijing, P.R. China

²School of Civil and Environmental Engineering, University of New South Wales, Sydney, NSW 2052, Australia

*Correspondence author: liuyangee@buaa.edu.cn

1. Introduction

□ Introduction

- In this work, evidence of large-scale ionospheric plasma depletion at middle and high latitudes over the USA during the intense storm on September 8, 2017, is discussed. We use both dense ground-based GNSS observables and SWARM ion-density measurements. The probable causes of such large-scale ionospheric responses are discussed.

2.Data and method

Data Representation

- OMNI: <https://omniweb.gsfc.nasa.gov/>
- ISGI: <http://isgi.unistra.fr/>

Ground observations

- CORS: <ftp://geodesy.noaa.gov/cors/>

Space-borne observations

- SWARM: <https://swarmdiss.eo.esa.int>

2.Data and method

□ Calculation of TEC

- The proposed TEC calculation method is referred to as the Ciraolo et al. (2007) arc-offset method and is realized by software provided by the T/ICTD Lab of the International Centre for Theoretical Physics.

$$VTEC = STEC \cdot \left[1 - \left(\frac{R_e \cos(\theta)}{R_e + H_{ipp}} \right)^2 \right]^{-\frac{1}{2}}$$

where R_e represents the average radius of the Earth, θ is the elevation angle in radians, and H_{ipp} denotes the average height of the IPP taken as 450 km.

Ciraolo, L., Azpilicueta, F., Brunini, C., Meza, A., Radicella, S. M. (2007). Calibration errors on experimental slant total electron content (TEC) determined with GPS. J. Geod., 81(2):111-120.

2.Data and method

□ Calculation of ROTI

- First, the rate of STEC variation, denoted by ROT, is preferably obtained first. Let the STEC retrieved at two adjacent epochs $k+1$ and k be denoted as $STEC_{k+1}$ and $STEC_k$, respectively, and let the time interval be Δt_k ; then, ROT is represented as

$$ROT = \frac{STEC_{k+1} - STEC_k}{\Delta t_k}$$

- The ROT index (ROTI) is then derived by taking

$$ROTI = \sqrt{\langle ROT^2 \rangle - \langle ROT \rangle^2}$$

Pi, X., Mannucci, A. J., Lindqwister, U. J., Ho, C. M. (1997). Monitoring of global ionospheric irregularities using the worldwide GPS network. Geophysical Research Letters, 24(18):2283-2286.

2.Data and method

□ Calculation of TID

- Savitzky-Golay filter is applied to detrend the data to remove the influences of the background TEC, since the travelling ionospheric disturbance (TID) has been observed to have a better resolution during different periods using the Savitzky-Golay detrending method.

$$TEC_{disturb} = SG[dTEC]$$

- where $dTEC$ denotes the differential TEC given as

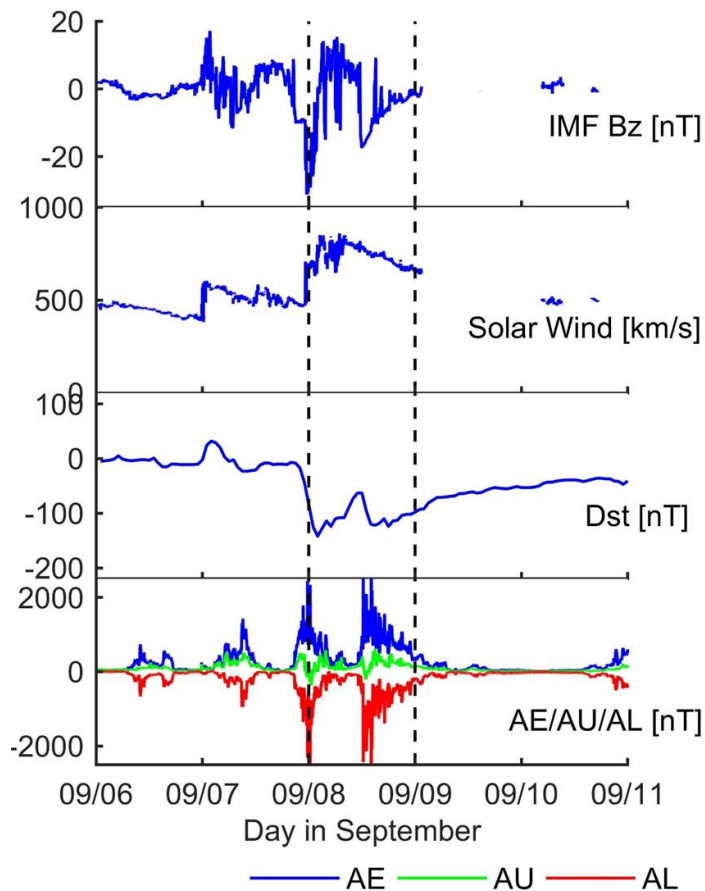
$$dTEC = STEC_{k+1} - STEC_k$$

- where STEC denotes the slant TEC observed from the IPPs.

Zhang, S.-R., Coster, A. J., Erickson, P. J., Goncharenko, L. P., Rideout, W., & Vierinen, J. (2019). Traveling ionospheric disturbances and ionospheric perturbations associated with solar flares in September 2017. *Journal of Geophysical Research: Space Physics*, 124.

3. Experimental results

□ the geomagnetic storm



The IMF Bz displayed perturbations and dropped to a minimum value of **-21.2 nT** with the second burst of solar wind. The IMF Bz oscillated with variations during September 8. The solar wind speed reached the maximum of **approximately 859 km/s**, maintained a high level for approximately 1 hour, and then decreased gradually. The maximum AU value was 620 nT on September 8 at 14:59 UT, and the minimum AL value was -2618 nT on September 8 at 00:18 UT. The maximum value of AE was **2677 nT** on September 8 at 14:06 UT. Dst dropped to its minimum value of **-142 nT** on September 8 at 02:00 UT. **The AE/AU/AL perturbations exhibited two sub-patterns during the storm.**

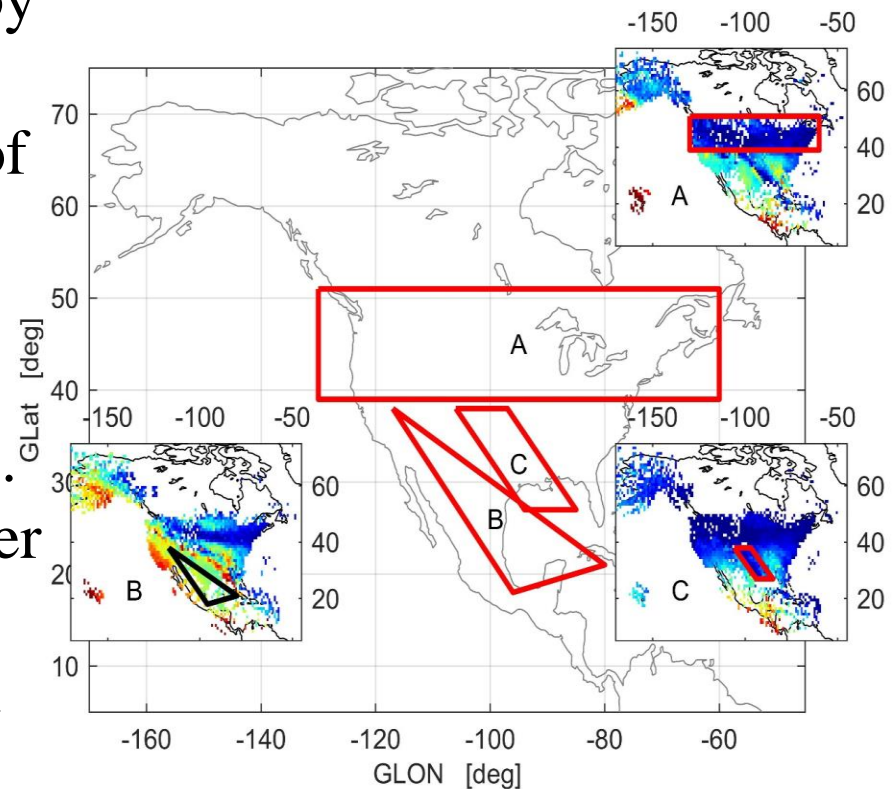
3. Experimental results

□ TEC fluctuations

Region A covers the area bounded by $70\text{-}130^\circ$ W and $30\text{-}50^\circ$ N and was probably caused by the movement of the mid-latitude density trough.

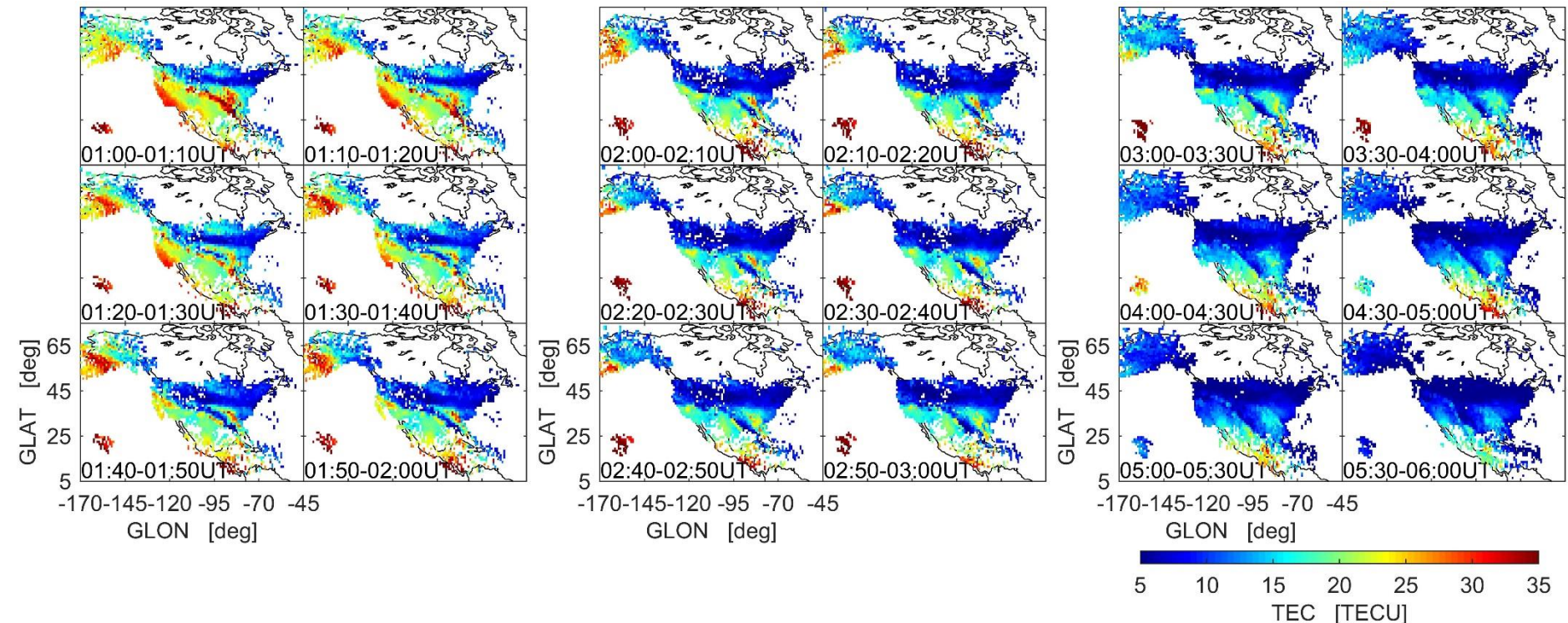
Region B, which covers the area of $75\text{-}120^\circ$ W and $15\text{-}35^\circ$ N, contained short-period irregularities.

Region C, which covers the area over $70\text{-}110^\circ$ W and $15\text{-}35^\circ$ N, was oriented more along the north-south direction and showed a classic negative storm response.



3. Experimental results

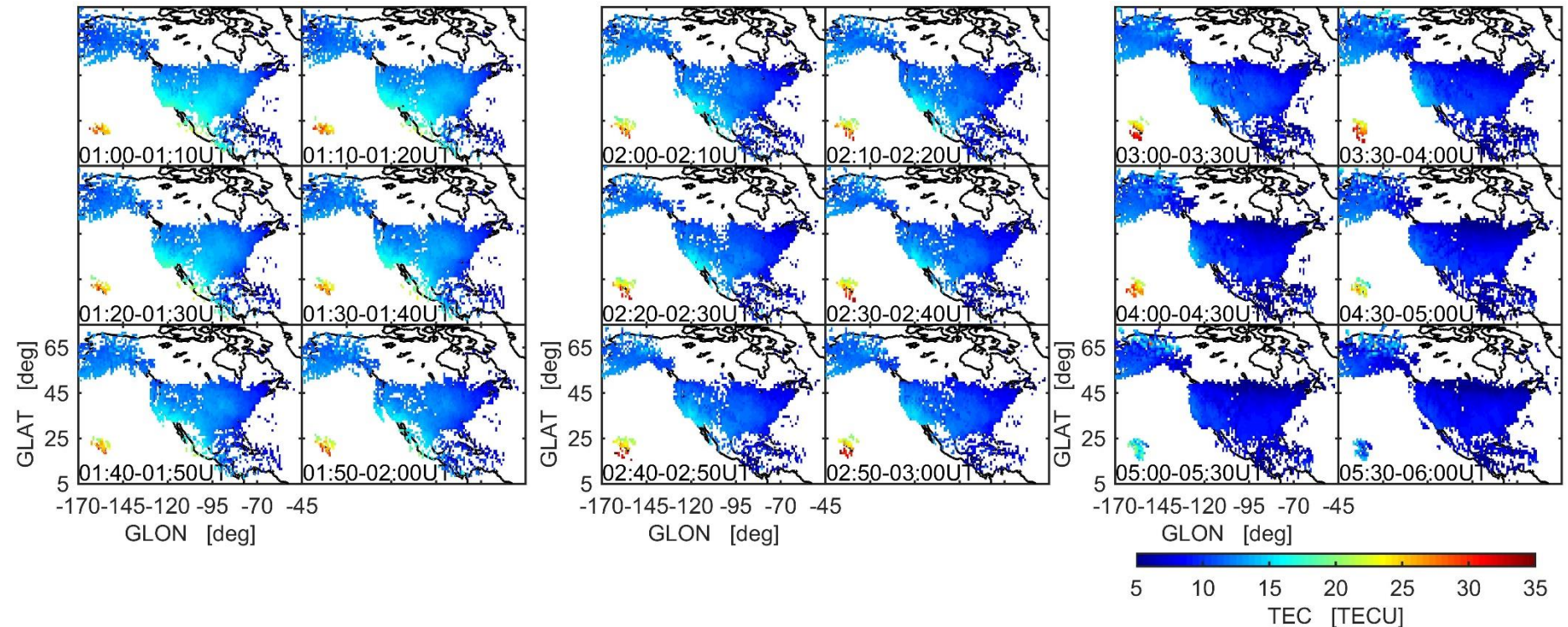
□ TEC fluctuations



The data come from the CORS network on September 8, 2017. Here, the TEC over the first 6 UT hours is demonstrated. The TEC map was generated in 10 min intervals during the first two hours and 30 min intervals from 03:00 UT to 06:00 UT. The geographical region spans the latitudes of $5\text{-}65^\circ$ N and the longitudes of $170\text{-}45^\circ$ W.

3. Experimental results

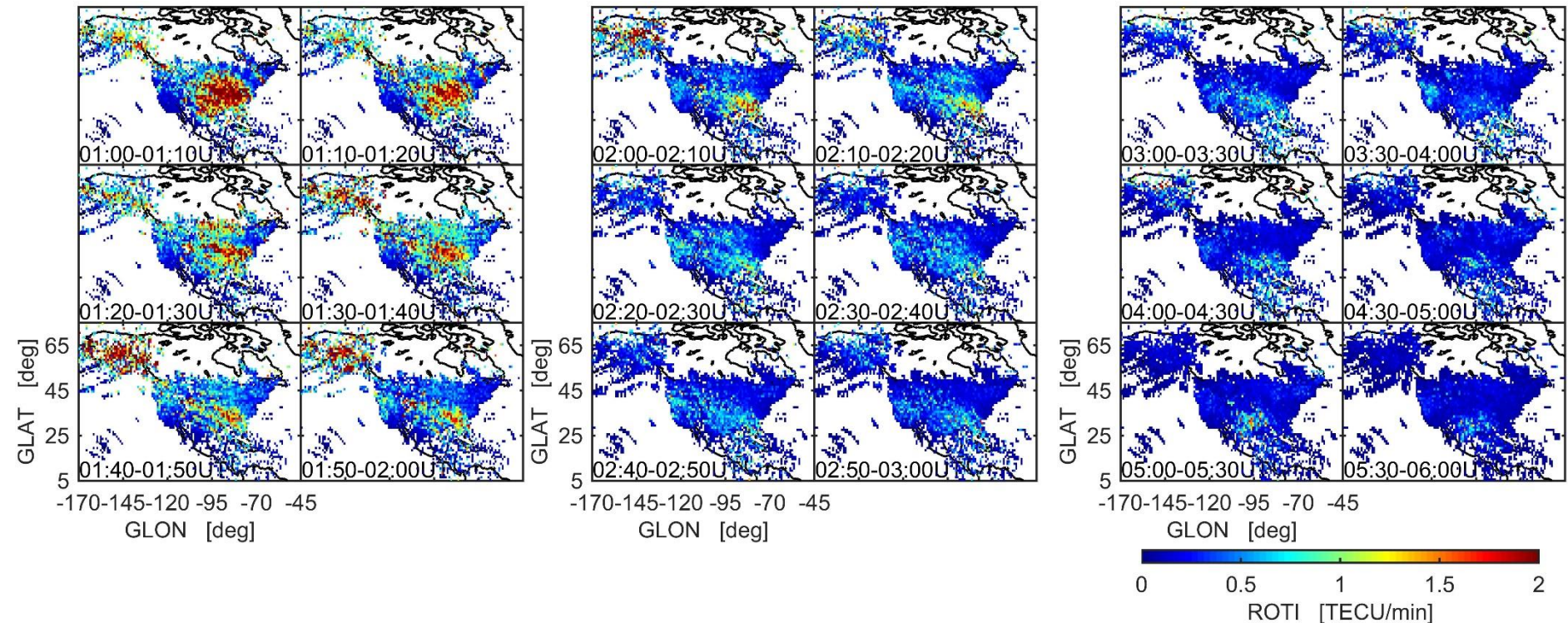
□ TEC Fluctuations



The data come from the CORS network on September 7, 2017. The TEC of the first 6 UT hours is demonstrated. The TEC map was generated in 10 min intervals during the first two hours and 30 min intervals from 03:00 UT to 06:00 UT. The colour bar indicates the intensity of TEC values, which range from 5 to 35 TECU.

3. Experimental results

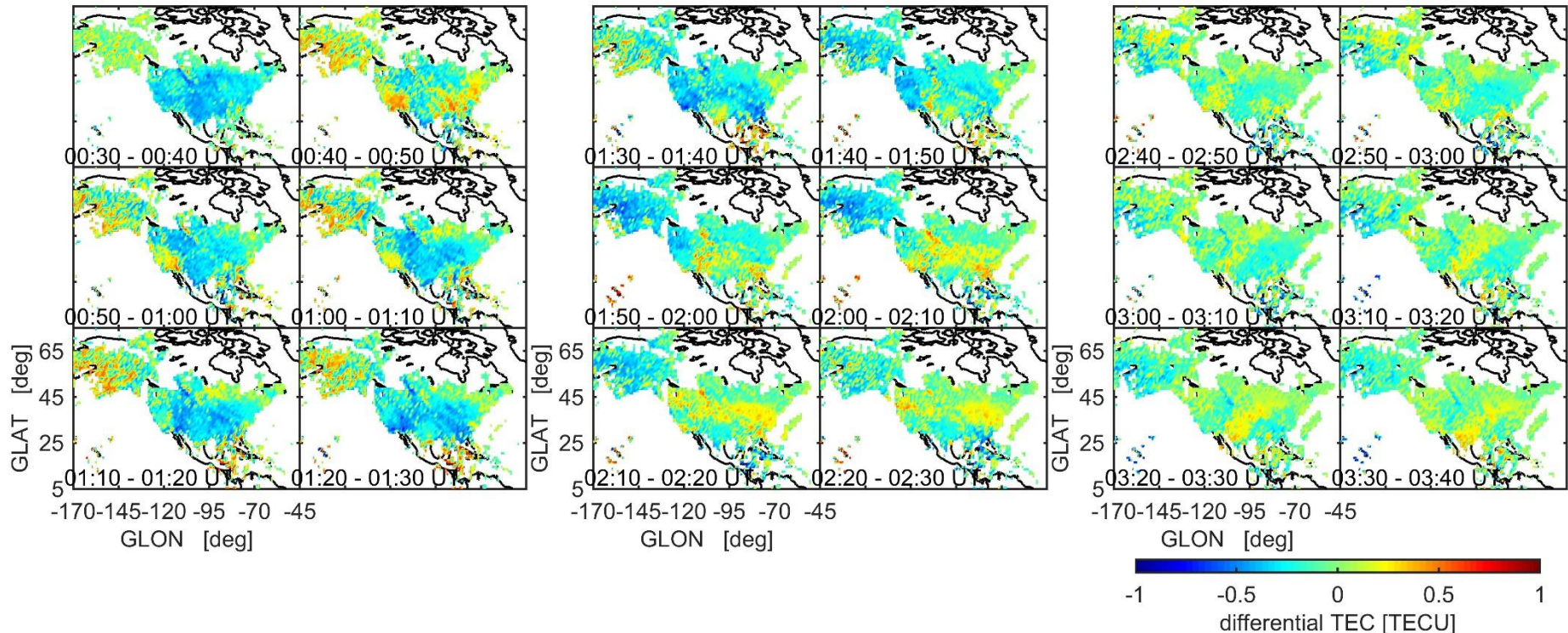
□ Response of ROTI



The data come from the CORS network on September 8, 2017. The ROTI values of the first 6 UT hours are computed. The ROTI map was generated in 10 min intervals during the first two hours and 30 min intervals from 03:00 UT to 06:00 UT. The colour bar indicates the intensity of the ROTI, which ranges from 0 to 2 TECU/min.

3. Experimental results

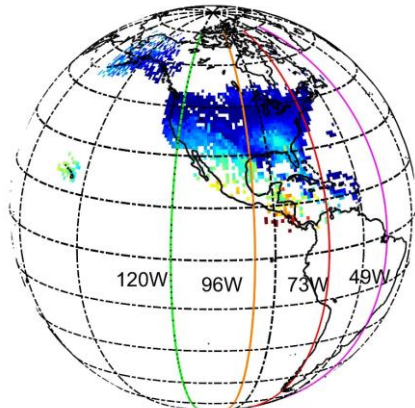
□ TID during the storm



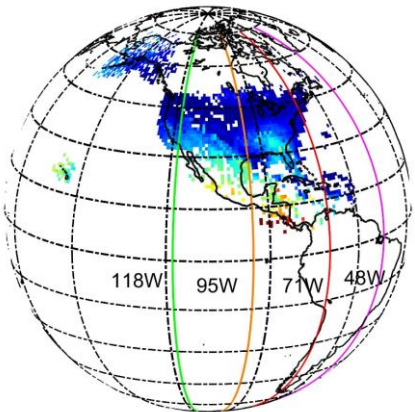
Top: TID in Alaska from 00:40 UT to 01:20 UT with a wavelength of over 800 km.
Middle: TID propagating in the poleward direction covering the longitudes of 70-110° W and the latitudes of 25-40° N from 01:50 UT to 02:30 UT. Bottom: TID propagating in the equatorward direction (southeast from Alaska to the middle and low latitudes of the contiguous USA).

3. Experimental results

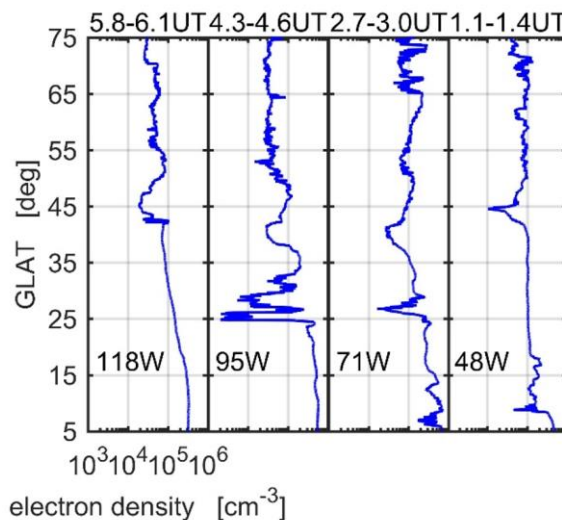
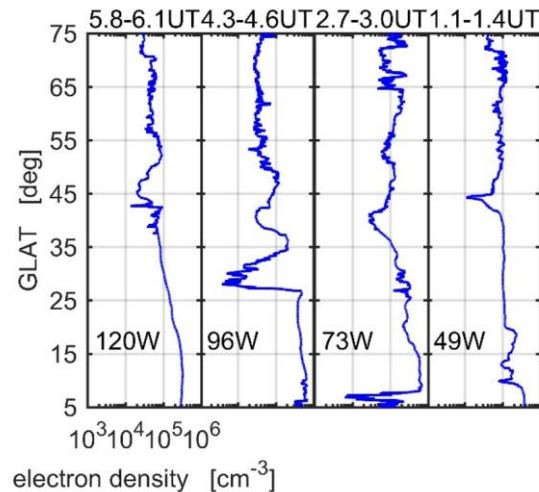
□ Ion-density perturbations



SWARM A



SWARM C



It is obvious that two paths from SWARM A and C (in red colour) separately pass through region C, as presented in previous slide. A strong electron density depletion is noticed in the region centred on 28° N, 96° W observed by SWARM A; the electron density was 3702 per cm⁻³ compared to the background value exceeding 10⁵ per cm⁻³. A similar feature is observed in the region centred on 25° N, 95° W observed by SWARM C; the electron density was 1990 per cm⁻³ compared to the background value exceeding 10⁵ per cm⁻³.

4. Conclusions

□ Conclusions

- During the main phase of the storm, a noticeable mid-latitude trough was observed from 40°N to 50°N ; the probable causes are the combination of a classic negative storm response with increments in the neutral composition and the expansion of the auroral oval, which pushed the mid-latitude trough equatorward.
- The depletion region covered a wide longitudinal extent of over 6000 km; the TEC trough extended equatorward and lasted for approximately 5 hours with an average TEC below 5 TECU.

4. Conclusions

□ Conclusions

- Ionospheric irregularities were also observed; super-scale plasma depletion was observed by SWARM data accompanied by the expansion of the mid-latitude trough.
- Two major factors were identified. The first is the PPEF from high latitudes, forming the TEC fluctuations in region B and further enhancing the ROTI.
- The second is a poleward neutral wind, which helps to decrease the electron density, leading to typical negative responses at high and mid-latitudes over the USA.

4. Conclusions

□ Conclusions

- An MSTID was revealed by the fluctuations of the differential TEC; the maximum fluctuation amplitude exceeded 2 TECU during 01:00 UT and 02:00 UT.
- It was supposed that the evolution of these super-scale plasma depletions probably contributed to the MSTID propagation from high latitudes to low latitudes, transporting high temperatures resulting from Joule heating, which can speed up the recombination efficiency of the ionosphere.

Liu, Y.; Li, Z.; Fu, L. ; Wang, J.; Zhang, C. Studying the ionospheric responses induced by a geomagnetic storm in September 2017 with multiple observations in America. *GPS Solut.* 2020, 24, doi:10.1007/s10291-019-0916-1.

Acknowledgment

□ Acknowledgments

- This work was supported by the National Natural Science Foundation of China Innovation Group 61521091 and National Natural Science Foundation of China under Grant 61771030, 61301087. The contribution is also supported by the 2011 Collaborative Innovation Center of Geospatial Technology.
- Special thanks to all providers of data used (OMNIweb from NASA Goddard Space Flight Center to provide IMF Bz, solar wind data; International Services of Geomagnetic Indices to provide Dst, AE/AU/ALdata , National Geodetic Survey to provide CORS GPS data, European Space Agency to provide SWARM data used in this research).

Thank you!